

# Catalytic Cooperation between a Copper Oxide Electrocatalyst and a Microbial Community for Microbial Electrosynthesis

Konstantina-Roxani Chatzipanagiotou,<sup>[a, b]</sup> Virangni Soekhoe,<sup>[a, b]</sup> Ludovic Jourdin,<sup>[b, c]</sup> Cees J. N. Buisman,<sup>[b]</sup> J. Harry Bitter,<sup>\*[a]</sup> and David P. B. T. B. Strik<sup>\*[b]</sup>

Electrocatalytic metals and microorganisms can be combined for CO<sub>2</sub> conversion in microbial electrosynthesis (MES). However, a systematic investigation on the nature of interactions between metals and MES is still lacking. To investigate this nature, we integrated a copper electrocatalyst, converting CO<sub>2</sub> to formate, with microorganisms, converting CO<sub>2</sub> to acetate. A co-catalytic (i.e. metabolic) relationship was evident, as up to 140 mgL<sup>-1</sup> of formate was produced solely by copper oxide, while formate was also evidently produced by copper and

consumed by microorganisms producing acetate. Due to non-metabolic interactions, current density decreased by over 4 times, though acetate yield increased by 3.3 times. Despite the antimicrobial role of copper, biofilm formation was possible on a pure copper surface. Overall, we show for the first time that a CO<sub>2</sub>-reducing copper electrocatalyst can be combined with MES under biological conditions, resulting in metabolic and non-metabolic interactions.

## Introduction

CO<sub>2</sub> is regarded as a potential feedstock for fuels, chemicals and materials.<sup>[1]</sup> However, the conversion of CO<sub>2</sub> is considered challenging, due to the thermodynamic stability of the molecule.<sup>[2]</sup> Therefore, energy is needed to convert CO<sub>2</sub>. Electricity-driven conversion of CO<sub>2</sub>, using renewable electricity (e.g. solar, wind) is particularly attractive, since it can convert intermittently-available electricity into chemical energy (i.e. fuels or chemicals from CO<sub>2</sub>), thus facilitating the storage and transportation of renewable energy.<sup>[3]</sup>

A technically and economically emerging technology for electricity-driven CO<sub>2</sub> conversion is Microbial Electrosynthesis (MES).<sup>[4]</sup> A schematic of this process is shown in Figure 1. Water is oxidized at the anode electrode (Figure 1, eq. I), releasing O<sub>2</sub>

gas, protons (H<sup>+</sup>) and electrons (e<sup>-</sup>). As illustrated in Figure 1, protons and electrons are transferred to the cathode side, via the electrolyte (blue arrows) and the external electric circuit (black arrows), respectively. At the cathode, whole cell microorganisms (e.g. autotrophic acetogenic or methanogenic bacteria), under pure, one-species cultures, or as mixed cultures, catalyse the conversion of CO<sub>2</sub>, under (or close to) ambient conditions in aqueous electrolytes<sup>[5]</sup> (Figure 1, eq. IV, VI, VII). MES microorganisms include electro-active species, which can directly take up electrons from the cathode electrode (i.e. direct electron transfer, Figure 1 pathway a), as well as microorganisms that rely on electrochemically provided mediators like hydrogen, formate or methyl viologen (i.e. mediated electron transfer, Figure 1 pathway c).<sup>[5]</sup> Among the possible electron donors for MES, a further distinction can be made between compounds that get recycled from the electrode to the microorganisms (such as methyl viologen), and compounds that get consumed by microorganisms, such as H<sub>2</sub> (an electron donor for the Wood-Ljungdahl metabolic pathway of acetate biosynthesis) and formate (a key intermediate of CO<sub>2</sub> reduction via this metabolic pathway).<sup>[6]</sup> End products of CO<sub>2</sub> reduction via MES are typically acetate (CH<sub>3</sub>COO<sup>-</sup>) and methane (CH<sub>4</sub>),<sup>[7]</sup> whereas multi-carbon components like butyrate and caproate have also been reported.<sup>[8]</sup> In addition, the microorganisms themselves grow during MES and are therefore a biobased source that could be refined for proteins and other microbial constituents.<sup>[9]</sup> The unique product spectrum, as well as the use of inexpensive, self-regenerating biocatalysts, give MES a distinct position compared to chemical electro(catalytic) synthesis.

MES production rates are often limited by the electron transfer rate from the electrode to the microorganisms.<sup>[10]</sup> One approach to improve this is to increase the concentration of electron donors for mediated electron transfer. For example,

[a] K.-R. Chatzipanagiotou, V. Soekhoe, Prof. Dr. J. H. Bitter  
Biobased Chemistry and Technology  
Wageningen University & Research  
Bornse Weiland 9, 6708 WG Wageningen (The Netherlands)  
E-mail: harry.bitter@wur.nl

[b] K.-R. Chatzipanagiotou, V. Soekhoe, Dr. L. Jourdin, Prof. Dr. C. J. N. Buisman,  
Dr. D. P. B. T. B. Strik  
Environmental Technology  
Wageningen University & Research  
Bornse Weiland 9, 6708 WG Wageningen (The Netherlands)  
E-mail: david.strik@wur.nl

[c] Dr. L. Jourdin  
Currently at Department of Biotechnology  
Delft University of Technology  
van der Maasweg 9, 2629 HZ Delft (The Netherlands)

Supporting information for this article is available on the WWW under  
<https://doi.org/10.1002/cplu.202100119>

© 2021 The Authors. ChemPlusChem published by Wiley-VCH GmbH. This is an open access article under the terms of the Creative Commons Attribution Non-Commercial License, which permits use, distribution and reproduction in any medium, provided the original work is properly cited and is not used for commercial purposes.

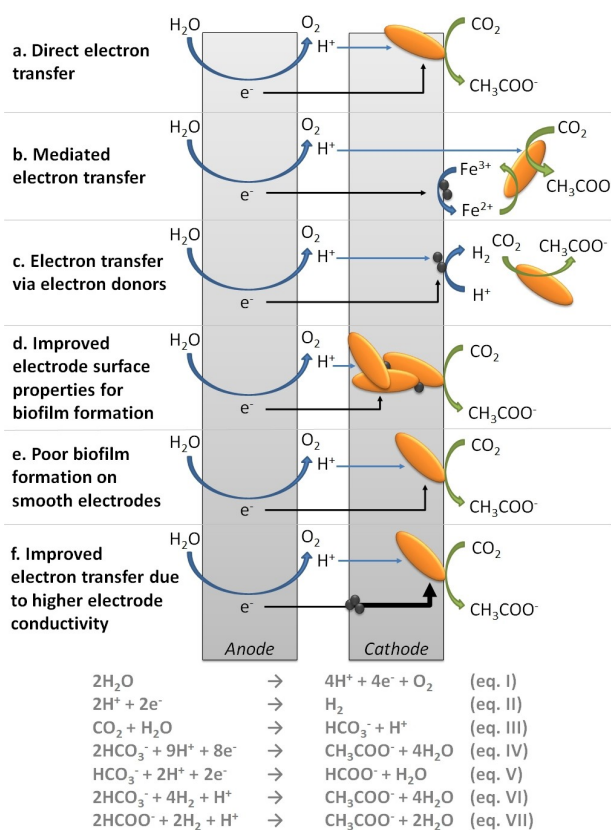


**Figure 1.** Schematic representation of the relationship between a metal catalyst (for example iron, illustrated as grey nanoparticles) and a MES culture (illustrated as orange cells). Microorganisms or extracellular enzymes can use electrons directly from the cathode (a), or via mediators, such as by oxidizing reduced metal species on the electrode (b). Metal nanoparticles can catalyze the electrochemical production of electron donors such as  $\text{H}_2$  (c, eq. II) or formate (eq. V), which can be used by planktonic microorganisms. Microorganisms utilize the  $\text{H}^+$  and  $\text{e}^-$  (or the  $\text{H}_2$  and formate), to convert  $\text{CO}_2$  (dissolved in the electrolyte, eq. III) to products such as acetate (eq. IV, VI and VII). Metal nanoparticles on the electrode can likely increase the surface area and porosity of the electrode, which improves biofilm formation (d), compared to unmodified, smooth electrodes (e). Metal nanoparticles can also likely increase the conductivity of the electrode (f), thus leading to improved electron transfer to the microorganisms.

biocompatible metal electrocatalysts have been recently developed, which achieve high-rate generation of  $\text{H}_2$ ,<sup>[10c,11]</sup> in order to increase the overall production rate of MES. As such, a syntrophic (i.e. metabolic) relationship is essentially developed between the  $\text{H}_2$ -producing metal catalysts and  $\text{CO}_2$ -reducing biocatalysts. A schematic representation of this relationship is shown in Figure 1 pathway c.

Mediated electron transfer via *in situ* generated electron donors would also expand the spectrum of potential microorganisms that can be used for MES to species which depend on  $\text{H}_2$  consumption, such as specific acetogenic and methanogenic microorganisms.<sup>[10c]</sup> Aside from syntrophic, non-metabolic effects may also arise from the combination of the two types of catalysts (i.e. symbiotic effects). Adding metals on an electrode before biofilm development likely affects the surface properties and conductivity of the cathode, which in turn can influence the electron transfer and biofilm attachment during MES

(Figure 1 pathways d-f).<sup>[12]</sup> While increasing the surface area and porosity of the electrode is considered to improve biofilm attachment, symbiosis between the two catalysts can also have negative effects. For example, some metals (e.g. metallic silver and copper and their oxides) can be toxic to microorganisms via several mechanisms, including causing structural changes to biological membranes, the formation of free radicals and reactive oxygen species, and interaction with enzymes, proteins and DNA, which leads to damage and deactivation.<sup>[13]</sup> Furthermore, microbial growth on a catalytic electrode could result in blocking of the catalyst's surface,<sup>[14]</sup> thus leading to loss of catalytic activity. In addition, microbial components and metabolites (e.g. sulfide and sulfate ions) in the electrolyte could result in catalyst poisoning.<sup>[15]</sup> It should be noted that the microbial growth medium of MES already contains trace metals like copper to support microbial growth. In previous studies on MES, copper deposits were found on the electrode surface after biofilm development, and it was suggested that microbial modification of the electrode surface (possibly via biological synthesis of catalytic nanoparticles from dissolved copper) enhanced the formation of hydrogen.<sup>[16]</sup> Thus, combining metal electrocatalysts and biocatalysts could affect MES performance via multiple mechanisms, including syntrophic and symbiotic effects.

Formate production has also been investigated to integrate electrocatalytic and microbial conversions. Practically, this can be of use because formate is an in-water-storable electron donor and provides a versatile substrate for formatotrophic organisms.<sup>[17]</sup> Earlier work of Li and co-workers<sup>[18]</sup> showed a first proof of principle for catalytic cooperation between a metal and bio-electrocatalyst, based on formate production by the metal catalyst and subsequent conversion by microorganisms. A pure culture of the chemolithoautotrophic bacterium *Cupriavidus necator* (formerly *Ralstonia eutropha*), genetically engineered to enable the conversion of formate to higher alcohols, was able to *in situ* convert formate that was electrocatalytically produced from  $\text{CO}_2$  by an indium cathode.<sup>[18]</sup> More recently, an indium electrocatalyst converting  $\text{CO}_2$  to formate was used as cathode, in combination with pure cultures of *Escherichia coli* strains, genetically engineered to enable the production of pyruvate from formate and  $\text{CO}_2$ .<sup>[19]</sup> Hegner and co-workers investigated the combination of Indium-electrocatalysed formate production and microbial utilization in a two-step reaction, wherein genetically engineered strains of *Methylobacterium extorquens* AM-1 were introduced in the reactor after formate production, and were able to deplete formate, forming mesaconate and methylsuccinate.<sup>[20]</sup> Similar studies have also been performed using non-genetically engineered microorganisms, namely *Methylobacterium extorquens* AM1 and *Cupriavidus necator* H16, to produce Poly(3-hydroxybutyrate) (PHB) from *in situ* electrochemically generated formate, in combination with an indium electrocatalyst.<sup>[21]</sup> These studies demonstrate that a syntrophic relationship based on formate between metal electrocatalysts and biocatalysts is possible in one reactor. However, other aspects of the apparent "symbiotic relationship" between the two catalysts (such as bio-toxicity or metal catalyst poisoning) were not addressed, and no evidence

is provided on the type of syntrophic relationship (i.e. mutualistic, wherein both species benefit; commensalistic, wherein one species benefits and other is not affected; or parasitic, wherein one species benefits and other is harmed).

We have previously shown a syntrophic relation between a copper oxide electrocatalyst and a mixed-culture of naturally-occurring microorganisms, using sequential reactors. Specifically, the copper oxide electrocatalyst produced formate from CO<sub>2</sub> within a microbial growth medium electrolyte, and this medium was thereafter transferred into bio-reactors, where microorganisms, H<sub>2</sub> and CO<sub>2</sub> were supplied. Microorganisms consumed the provided substrates (formate, H<sub>2</sub> and CO<sub>2</sub>) and produced acetate and methane.<sup>[22]</sup> The objective of the present follow-up study is to investigate potential symbiotic and syntrophic effects, by combining either non-formate producing copper foil (Cu-foil) or formate-producing copper oxide (CuOx) electrodes with biocatalysts together in one MES reactor with continuous CO<sub>2</sub> supply. Emphasis was given on electrocatalytically produced formate-based electron transfer interactions (Figure 1 pathway c), since formate is highly soluble in water and therefore its dynamics could be monitored in the experimental approach used.

Copper is among the best electrocatalysts which demonstrate formate production at high selectivities.<sup>[23]</sup> As a catalyst, and particularly in combination with microbial catalysis, copper is a controversial material, due to its known toxic effects,<sup>[24]</sup> as well as its potentially negative environmental impact, either during the extraction of copper,<sup>[25]</sup> or due to leaching and subsequent release to the environment.<sup>[26]</sup> However, for CO<sub>2</sub> electroreduction, copper is unique among metal catalysts, as it can produce a variety of products besides formate at high current efficiencies, such as methanol, ethylene and ethanol.<sup>[27]</sup> Therefore, a proof-of-principle of catalytic cooperation between naturally-occurring microorganisms and copper may allow to envision various co-catalytic routes, based on the unique product spectrum of copper, for final products of longer carbon chains and with higher value, compared to acetate and methane, such as butyrate, isobutyrate,<sup>[28]</sup> caproate,<sup>[29]</sup> and caprylate.<sup>[30]</sup> Furthermore, several methods have been described to recover copper from waste,<sup>[31]</sup> including the synthesis of catalysts from waste.<sup>[32]</sup> Particularly the use of copper as a cathodic electrocatalyst could possibly further decrease the environmental impact due to leaching, as copper can be recovered from the electrolyte via electrodeposition.<sup>[22]</sup> Taken together, while an impact analysis of the use of copper was not part of this study, copper is expected to be a promising catalyst for the development of co-catalytic concepts in combination with microbial catalysts.

In the present study, inoculation of the reactors containing copper electrodes with the bio-electrocatalyst led to growth of microorganisms, which produced acetate as the final product. In the presence of both CuOx and biocatalysts, formate was most evidently produced by the metal electrocatalyst, and consumed by microorganisms, to produce the acetate. By comparing the performance of each copper electrode with and without microorganisms, differences were observed in current density for both electrodes, as well as the catalytic activity of

the copper foil electrode. In addition, differences in microbial acetate production were observed among reactors with Cu-foil and CuOx electrodes. Another remarkable finding was the formation of biofilm on the copper electrodes. While biofilm formation on other metal electrodes has been previously shown, we will show for the first time here that pure copper electrodes can serve as a bio-cathode, despite its known antimicrobial role.<sup>[24]</sup> Overall, these results show novel MES integrations, by combining a copper oxide or a plain copper foil electrode with microorganisms in one reactor.

## Results

### Electrochemical experiments

#### *Effect of catalytic combination on current density*

In order to investigate the potential syntrophic and symbiotic effects between metal and biocatalysts, four types of electrochemical experiments were performed, namely: abiotic copper electrosynthesis (CES) in fresh electrolyte, microbial electrosynthesis with copper electrodes (MES), copper electrosynthesis in the presence of deactivated microorganisms (deactivated MES), and microbial electrosynthesis with copper electrodes in reactors with pre-grown biocatalyst on a graphite felt electrode (mature MES). The current density recorded during different electrochemical experiments is shown in Figure 2a for CuOx and Figure 2b for Cu-foil electrodes. Data for deactivated MES experiments with Cu-foil are not available in duplicate, and the results of a single experiment are shown in Supporting Information (Figure S1).

Within minutes after applying a negative cathode potential, the current density rapidly decreased for all CuOx electrodes (e.g. from  $-2.6$  to  $-1.3$  mAcm<sup>-2</sup> for CES experiments in Figure 2a), while this trend was not observed with Cu-foil electrodes (Figure 2b, Figure S1). A sharp peak in the current density of the CuOx electrode was observed on day 1 during the CES experiment (Figure 2a). This was likely due to unintentional perturbation while sampling, as it was not observed in any other experiment with CuOx or Cu-foil electrodes.

Within the first five days, a different pattern could be observed for current evolution among experiments with fresh (CES, MES) and used electrolyte (mature and deactivated MES, Figure 2a,b, Figure S1). For both electrodes, during CES experiments, the current density increased and thereafter decreased to less negative values, followed by a second decrease. Thus, two opposite peaks were formed over time, i.e. towards more negative values (around day 1) and towards more positive values (around day 3). In MES experiments, the current density also increased and thereafter decreased, but this transition was slower compared to CES experiments.

Only one peak towards more negative values could be distinguished around day 3 during MES experiments. On the contrary, during experiments in used electrolyte (deactivated and mature MES), a more stable current density was recorded

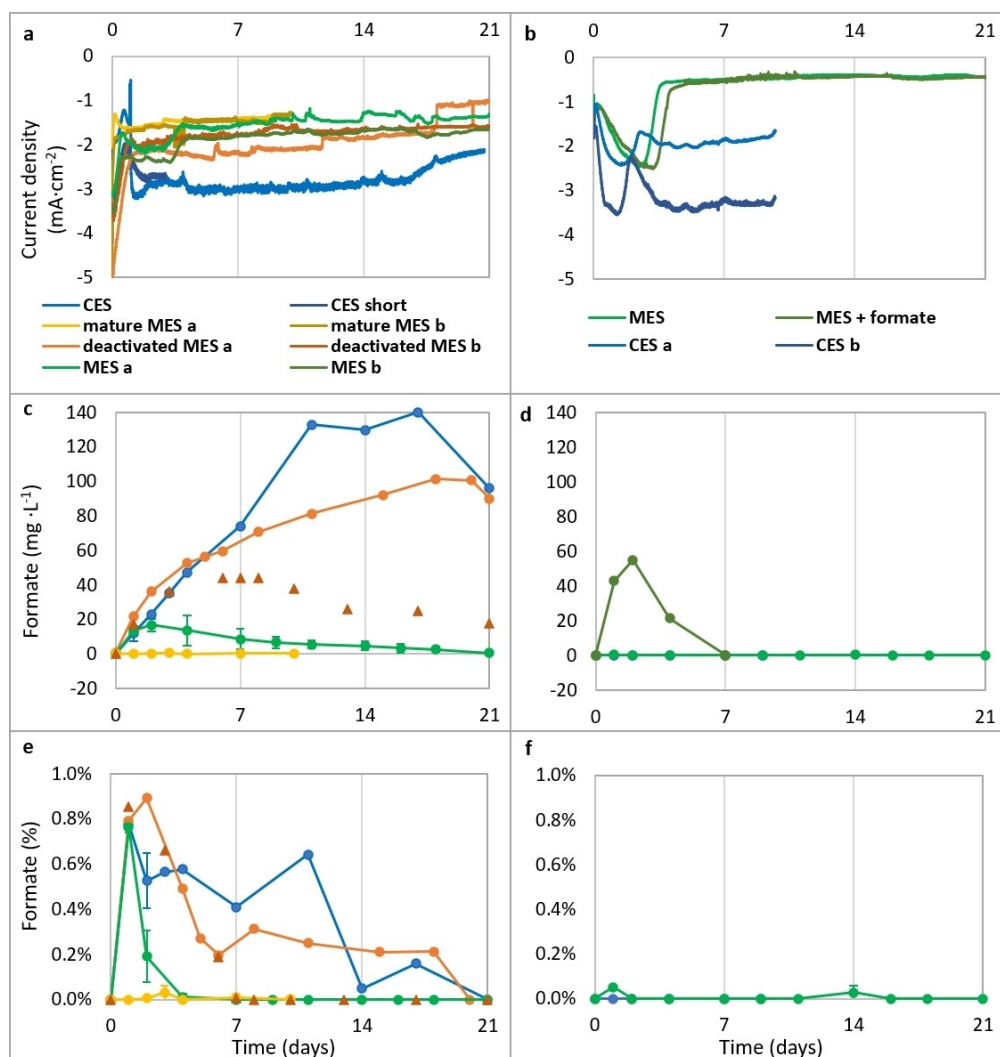


**Figure 2.** Electrochemical performance of CuOx (left) and Cu-foil (right) electrodes during various chronoamperometry experiments. a, b: current density; c, d: dissolved formate concentration; and e, f: calculated electron recovery over time. When available, error bars indicate standard deviation based on duplicate experiments. For CES experiments with CuOx, due to biological contamination in one reactor, data for long-term operation are not available in duplicate. Instead, data from a short-term abiotic experiment are shown, which has been previously reported,<sup>[22]</sup> to illustrate the reproducibility among experimental repetitions. For deactivated MES experiments, results of the duplicate reactor that became contaminated are shown separately (as ▲) in Figure c and e.

during the first 5 days, and no clear peaks could be observed over time with either CuOx or Cu-foil electrodes.

Compared to the first three days of operation, during which fluctuations in the current could be observed, by day 5 the current density had become more stable in all experiments (i.e. steady state), and slowly decreased to less negative values over time for both electrodes (Figure 2a,b). The approximate time to reach this steady-state (based on visual evaluation of the provided graphs), as well as the current density during steady state, was different among experiments. For an easier comparison, a summary of the steady-state current density for all experiments is given in Table 1. Irrespective of the experiment (e.g. CES, MES or deactivated MES tests), the time to reach steady state was the same between CuOx and Cu-foil electrodes and corresponded to approximately 4.5 days in fresh electrolyte (CES, MES), and up to 2 days in spent electrolyte (mature and deactivated MES) (Table 1). For both CuOx and Cu-foil electro-

**Table 1.** Overview of current densities recorded with CuOx and Cu-foil electrodes during chronoamperometry experiments at different conditions.

Experiment	CuOx Average current density <sup>[a]</sup> [day 4–7] [mA cm <sup>-2</sup> ]	Time until stable current [days]	Cu-foil Average current density <sup>[a]</sup> [day 4–7] [mA cm <sup>-2</sup> ]	Time until stable current [days]
CES	$-2.63 \pm 0.04$	4.5	$-2.67 \pm 0.05$	4.5
deactivated MES	$-1.79 \pm 0.03$	2	$-0.87 \pm 0.03$	2
MES	$-1.73 \pm 0.13$	5	$-0.56 \pm 0.06$	5
mature MES	$-1.45 \pm 0.02$	0.5	n.a.	n.a.

[a] Current density was calculated by first calculating the average current density of each experiment at every time point based on duplicate reactors, and thereafter calculating the average and standard deviation for all time points between day 4 and 7.



des, a more negative current density was recorded during CES experiments (i.e. up to  $-2.6 \text{ mA cm}^{-2}$  at steady state), compared to all experiments with microorganisms in the electrolyte (up to  $-1.8 \text{ mA cm}^{-2}$  for CuOx). Particularly for Cu-foil, the average current density between days 4–7 was 4.8 times higher during CES, compared to MES experiments (Table 1). Differences in current density were also observed between the two electrodes in some experiments. Compared to Cu-foil, CuOx resulted in more negative steady-state current density during both MES ( $-1.73$  compared to  $-0.56 \text{ mA cm}^{-2}$ ) and deactivated MES experiments ( $-1.79$  compared to  $-0.87 \text{ mA cm}^{-2}$ ). Instead, in the absence of bacteria (CES experiments), the steady state current density among the two electrodes was very similar (Table 1).

### Effect of the biocatalyst on formate concentration

Combining biocatalysts with copper electrocatalysts may lead to different patterns of formate concentration, resulting for example from the effect of the added biomolecules on the surface properties of the electrode (i.e. adsorption or blocking of catalytic surface), or the consumption of formate by microorganisms, which would effectively decrease the formate concentration. To compare the catalytic activity of copper among experiments, the concentration of formate produced and the calculated electron recovery are shown in Figure 2c and e, respectively.

For CuOx, both CES and deactivated MES experiments showed an increase of formate concentration over time until day 17, and thereafter a decrease by day 21 (Figure 2c). The calculated electron recovery into formate reached a maximum of approximately 0.8% within the first two days (Figure 2e), and remained above zero until day 17. The low electron recovery towards formate was likely due to the electrolyte composition, containing phosphate buffer, which has been previously shown to decrease the selectivity towards formate, compared to bicarbonate buffer.<sup>[22]</sup> The formate concentration and calculated electron recovery is in agreement with our previously reported findings for abiotic experiments with duration of 72 hours.<sup>[22]</sup>

Some deviations can be observed between CES and deactivated MES experiments, which cannot be further evaluated, due to the lack of duplicate data. Nevertheless, it can be postulated that deactivated MES effluent did likely not lead to deactivation or poisoning of the CuOx catalyst, and long-term catalytic activity of up to 18 days was retained with this electrolyte. Formate was the only liquid product detected during abiotic experiments with either CuOx or Cu-foil electrodes. Instead, gaseous products were formed with both electrodes, as was evident by gas bubble formation on the surface of both CuOx and Cu-foil during these experiments. Gas formation likely accounts for the remaining electron recovery during abiotic experiments.

While formate production with CuOx continued for multiple days in the absence of bacteria, a different pattern can be observed during MES and mature MES experiments (Figure 2c). Using CuOx catalyst, formate concentration increased until day

2 during MES, and thereafter gradually decreased, until formate was depleted on day 21. The calculated electron recovery to formate (Figure 2e) reached a maximum of about 0.8% on day 2, and thereafter also decreased to zero within the first 4 days. In the presence of a mature MES bio-culture, only trace amounts of formate could be detected in the electrolyte over time, corresponding to an electron recovery of less than 0.05%.

Formate concentration and electron recovery were also measured in reactors with Cu-foil electrodes (Figure 2d and f, Figure S1b and c, respectively). Measurable amounts of formate were produced with Cu-foil during deactivated MES experiments. The formate concentration increased until day 13, and the calculated electron recovery was  $>0$  during the first 13 days of the experiment (Figure S1). On the contrary, no formate production was detected with Cu-foil electrodes during CES experiments in fresh electrolyte at the same cathode potential ( $-1.2 \text{ V}$ , Figure 2d). In fact, electrocatalytic formate production with Cu-foil in fresh electrolyte was only detected at more negative potentials ( $-1.6 \text{ V}$ ), during additional abiotic experiments presented in Supporting Information (Figure S2). Therefore, compared to fresh electrolyte, deactivated MES effluent apparently decreased the over-potential for formate production with Cu-foil electrodes. During MES, trace amounts of formate could be detected in the electrolyte on days 1, 14 and 24, which were thereafter depleted (Figure 2d). Increase of formate concentration at those time points resulted in a positive value for the calculated electron recovery for Cu-foil on the corresponding days (Figure 2f).

### Effect of copper electrodes on microbial growth and metabolism

The concentration of acetate in the electrolyte and the calculated electron recovery was measured over time during MES and mature MES experiments, and the results are shown in Figure 3a and b, respectively. The concentration of formate during MES experiments with CuOx is also shown in this Figure (i.e. same as in Figure 2c), to better illustrate the simultaneous production and consumption of the two compounds over time during MES experiments.

No acetate production was detected with either copper electrode during CES experiments, thus confirming that acetate was produced by microorganisms. With both Cu-foil and CuOx electrodes, measurable amounts of acetate could be measured in the electrolyte during MES experiments by day 21. Thereafter, acetate concentration increased for both electrodes until the end of the experiment, with 3.3 times higher final concentration in the CuOx reactors (up to  $900 \text{ mg L}^{-1}$ ) compared to Cu-foil ( $270 \text{ mg L}^{-1}$ , Figure 3a). Nevertheless, the calculated electron recovery to acetate over time for both electrodes was similar (Figure 3b). Electron recovery became positive on day 21, when acetate production began, and increased to a maximum of about 30% for both electrodes on day 28. Thereafter, electron recovery to acetate decreased in all MES reactors until the end of the experiment (Figure 3b).

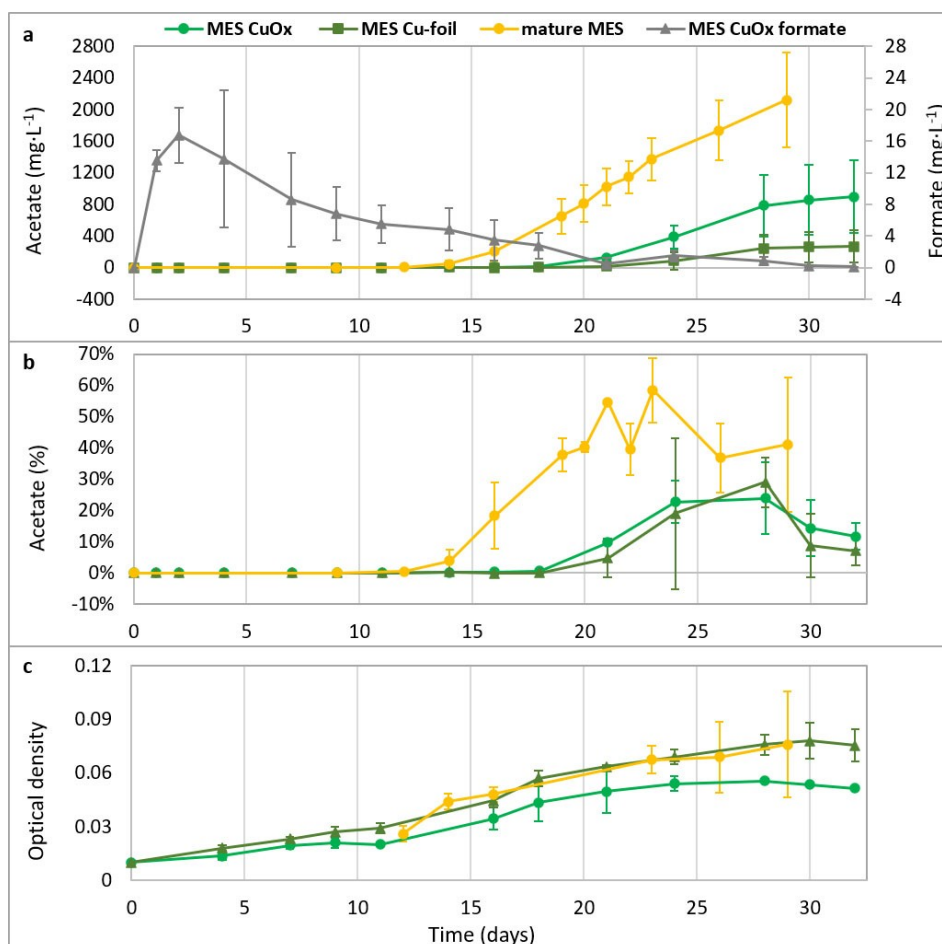


**Figure 3.** Bio-electrochemical performance during various chronoamperometry experiments. a: dissolved acetate concentration; b: calculated electron recovery; and c: optical density in the catholyte over time. For an easier comparison between Figures, in Figure 3a, the average concentration of formate is also shown during MES experiments with CuOx (i.e. same as in Figure 2c). Error bars indicate standard deviation based on duplicate experiments. During mature MES experiments, reactors were operated with graphite felt electrodes for 19 days at  $-1.06$  V vs. Ag/AgCl, until acetate production was observed. Thereafter, CuOx electrodes were added in these reactors, operating at  $-1.2$  V vs. Ag/AgCl for the rest of the experiment.

During mature MES experiments (Figure 3a), acetate was first detected in the electrolyte on day 14, and thereafter increased over time until the end of the experiment. The calculated electron recovery to acetate followed the same trend, increasing until day 21 to 55%, and thereafter fluctuated between 40% and 60% until the end of the experiment. Compared to MES experiments, which reached a maximum acetate concentration of  $0.78$  gL<sup>-1</sup> by day 28, acetate production was roughly 3 times higher with a mature MES biocathode, reaching a concentration of up to  $2.1$  gL<sup>-1</sup> by day 29 (Figure 3a). Acetate production was detected earlier in these reactors (day 14 compared to day 21), and thereafter the concentration increased over time until the end of the experiment. Higher acetate production by a mature MES bio-reactor was also evident based on the calculated electron recovery (Figure 3b). Compared to MES experiments, electron recovery was higher during mature MES experiments at every time point, reaching a maximum of 60% on day 23.

The optical density (OD) was measured in the electrolyte over time in all biological reactors, as an indicator of growth for

planktonic microorganisms (Figure 3c). Increase of OD in both MES reactors was evident already on day 4, and thereafter OD increased with time until the end of the experiment. Compared to CuOx electrodes, OD was higher at every time point during MES experiments with Cu-foil electrodes. A similar increase in OD over time was also observed during mature MES experiments.

#### Metabolic deactivation of MES with heat treatment

In order to confirm that deactivation of microorganisms was successful during deactivated MES experiments, acetate concentration and optical density (OD) were monitored in the electrolyte over time, as indicators of biological growth. The concentration of acetate is shown in Supporting Information (Figure S3).

The concentration of acetate during deactivated MES experiments decreased over time in both reactors, which could be due to evaporation and/or transport and oxidation at the

anode. Lack of acetate production supports that deactivation of microorganisms by heat treatment of the effluent was successful in these reactors. Optical density was not measured at every time point, as the sample volume required for continuous measurement could result in depletion of the electrolyte. Nevertheless, similar optical density values were measured at the start and at the end of the experiment ( $0.078 \pm 0.005$ ), thus further supporting the effective deactivation of microorganisms, as no growth of planktonic microorganisms was observed.

### Biofilm growth on pure copper electrodes

Characteristic SEM images of selected electrodes before and after operation are shown in Figure 4. Electropolished copper foil had a smooth surface before electrochemical testing (Figure 4a), but some heterogeneity and defects of unknown origin could be observed (i.e. black spots). Unused CuOx electrode surface was instead homogeneously covered with copper oxide particles (Figure 4b).

For CuOx electrodes after MES experiments, large flower-like crystals were observed with SEM (Figure 4d–e), which consisted of copper phosphate, as confirmed with EDX analysis. Crystals were likely formed during the fixation of SEM samples in glutaraldehyde, as similar crystal structures were also observed on unused CuOx electrodes stored in glutaraldehyde (not shown).

By the end of the MES experiment, the surface of Cu-foil was covered with biofilm, which appears as bright-coloured structures on the grey (copper) background (Figure 4c). Similar structures were observed on the surface of CuOx (Figure 4d–e), confirming biofilm growth on both electrodes the end of the experiment. The surface of Cu-foil was rather homogeneously

covered with biofilm structures (Figure 4c). Instead, on CuOx electrodes, the biofilm coverage appears more heterogeneous, as biofilm could be observed both on and among the copper phosphate crystals (Figure 4e). Higher magnification images obtained between the crystals reveal extensive formation of biofilm on the CuOx electrode, with a layer of microorganisms completely covering the electrode surface (Figure 4f). Nevertheless, a quantitative comparison of biofilm coverage between the two electrodes cannot be performed, as crystal formation on CuOx has significantly changed the surface structure.

## Discussion

### Symbiotic effects of microorganisms on copper electrodes

By comparing the current density among different experiments, the symbiotic, rather than syntrophic effects of microorganisms on the copper electrodes can be revealed, as will be further explained in this section.

The current density recorded over time during electrochemical experiments is shown in Figure 2a (for CuOx) and b (for Cu-foil). While a lot of different patterns emerge during the experiments, the current evolution can be roughly divided into three phases. The initial phase, during the first minutes of the experiment after a cathode potential is applied, is characterized by a sharp decrease in the current density from negative to less negative values for CuOx electrodes. This is likely associated with reduction of the surface metal oxide layer, and the same trend is not observed with Cu-foil electrodes (Figure 2b, Figure S1a).

The second phase lasts until approximately day 5, and is characterized by peaks in the current density during CES and MES experiments. Finally, after day 5, the current density for all electrodes reached a steady state phase, and slowly decreased until the end of the experiment. The average current density during steady state, and the time required to reach steady state for each experiment are also summarized in Table 1 (in Results). The use of fresh electrolyte resulted in a distinct pattern for current evolution until day 5 during experiments in fresh electrolyte (CES and MES), whereas this was not observed during experiments with spent electrolyte (mature and deactivated MES) (Figure 2a–b, Figure S1a). We have previously reported this characteristic pattern for current evolution in microbial growth medium, compared to buffer electrolytes, likely due to added nutrients and trace elements that get reduced or electrodeposited on the electrode surface at variable rates when negative cathode potential is applied.<sup>[22]</sup> During mature and deactivated MES experiments, the electrolyte was not fresh, but had instead been used electrochemically during experiments with graphite felt electrodes. Compounds that can act as electron sinks may have been already reduced during the initial operation. Lack of this characteristic pattern of current consumption during mature and deactivated MES experiments could therefore be due to the unavailability of reducible substrates in these spent MES electrolytes. Alternatively, the different pattern of current flow for both electrodes between

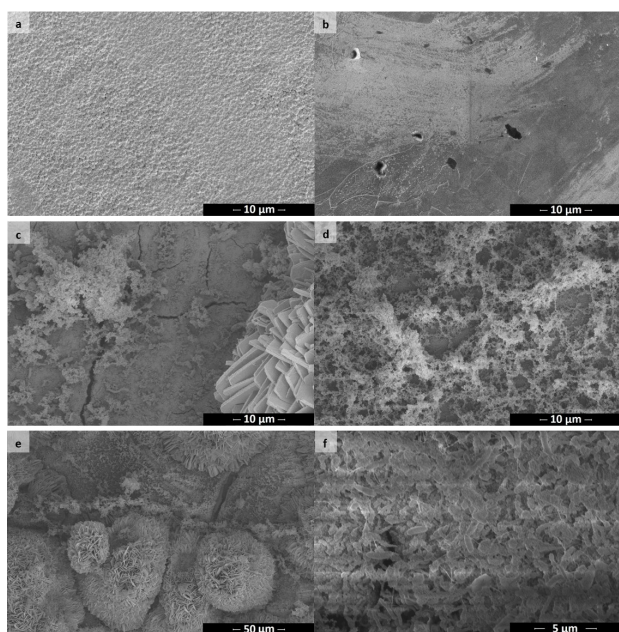


**Figure 4.** SEM images of electrodes before use (a: CuOx; b: Cu-foil) and after use (c, e, f: CuOx; d: Cu-foil) in MES experiments.

fresh and spent electrolyte could be due to the presence of (deactivated) microorganisms in the latter, but the exact mechanism cannot be elucidated based on the available data.

For both CuOx and Cu-foil, the average current density was lower in the presence of microorganisms, compared to the current recorded during abiotic experiments (Table 1). In fact, for each electrode type, the current density was similar in the presence of both metabolically active microorganisms (MES) and deactivated MES experiments (i.e. around  $-1.75 \text{ mA cm}^{-2}$  for CuOx electrodes and less than  $-1 \text{ mA cm}^{-2}$  for Cu-foil electrodes in both MES and deactivated MES experiments), and lower compared to CES experiments ( $-2.65 \text{ mA cm}^{-2}$  for both electrodes at steady state). In the presence of both active (MES) and inactive microorganisms (deactivated MES), the CuOx layer resulted in an increased average current density, compared to Cu-foil electrodes. On the contrary, the two electrodes produced similar current densities in the presence of fresh electrolyte (Figure 2a–b, Table 1). These observations support that microorganisms present in the electrolyte have an effect on the current density for both CuOx and Cu-foil electrodes. The effect was similar in the presence of active and metabolically-deactivated microorganisms, thus indicating a symbiotic, rather than a syntrophic (i.e. metabolic) effect. The effect of microorganisms on the recorded current density could be due to structures on the cytoplasmic membrane of microorganisms, such as phospholipids<sup>[33]</sup> and proteins,<sup>[34]</sup> which may interact with the surface of the electrode, or with compounds present in the electrolyte, such as sulphur-containing compounds,<sup>[35]</sup> which could result in catalyst poisoning. On the other hand, biogenic components present in the electrolyte may also explain the positive effect on the catalytic activity of Cu-foil during deactivated MES experiments, which, compared to CES experiments, exhibited a lower overpotential for formate production (Figure S1b, c). This could be due to organic or sulphur constituents acting as promoters,<sup>[36]</sup> thus improving the selectivity for formate production with Cu-foil, or the role of enzymes, which may get released in the electrolyte by the microorganisms during microbial growth or due to cell lysis upon deactivation of MES microorganisms, and catalyse formate production in deactivated MES experiments with Cu-foil.<sup>[37]</sup> Nevertheless, as characterization of the electrolyte components was not performed after the experiment, such hypotheses cannot be further substantiated at this stage.

### Syntrophic and symbiotic effects of copper on microorganisms

By comparing several parameters related to microbial growth among different experiments with the two types of copper electrodes, both syntrophic and symbiotic effects are evident between the two catalysts, and these effects will be further explained in this section.

Upon combining copper electrodes with MES, growth of microorganisms was evident in all biological reactors, as indicated by the increase of optical density (OD) in the electrolyte over time (Figure 3c). Dissolved  $\text{NH}_4$ , a major nutrient

for biological processes, was also measured in the electrolyte at certain time points during MES experiments (not shown in Figure 3), as an indicator of biological growth. While OD gives an indication only of planktonic microorganisms' growth,  $\text{NH}_4$  consumption is a measure of growth for both planktonic and biofilm-forming microorganisms. Decrease in  $\text{NH}_4$  concentration over time in all biological reactors further supports that growth of microorganisms was successful.

A clear difference can be observed in terms of microbial growth between the two electrodes during MES experiments. OD was higher in the case of Cu-foil compared to CuOx electrode at every time point during MES experiments, which implies that more planktonic bacteria were present in the reactors with Cu-foil, compared to CuOx. Additionally, lower  $\text{NH}_4$  concentration was also recorded in the presence of Cu-foil electrodes ( $22 \pm 0.4 \text{ mg L}^{-1}$ ), compared to CuOx electrodes ( $30.4 \pm 1 \text{ mg L}^{-1}$ ) on day 18. Thereafter, more  $\text{NH}_4$  was added to reactors with Cu-foil, to equalize the concentration among all reactors. In agreement with the OD results, increased consumption of  $\text{NH}_4$  with Cu-foil electrodes further supports that there was higher biomass growth in the presence of Cu-foil, compared to CuOx.

Compared to the long-term abiotic experiment, which showed that formate production with CuOx continued for 17 days after the start of the experiment, the calculated electron recovery of CuOx catalyst for formate dropped to zero within 4 days in the presence of microorganisms during MES experiments (Figure 2e). We have shown that long-term catalytic activity of CuOx (i.e.  $\text{CO}_2$  conversion to formate) is not evidently affected in the presence of deactivated biological effluent (Figure 2e). The decreasing formate concentration over time in biological reactors, which results in decrease of the calculated electron recovery, is therefore not attributed to a symbiotic, but rather a metabolic (i.e. syntrophic) effect, such as formate consumption by the biocatalyst.

Consumption of formate in the CuOx reactor during the first 18 days of MES experiments was not accompanied by acetate production (Figure 3a). Nevertheless, OD increase (Figure 3c) reveals there was biological activity in all reactors already on day 4. Therefore, formate was likely used by the microorganisms as a carbon and electron source for other biological processes during this time, such as cell division. Formate depletion by the biocatalyst can also be observed during mature MES experiments. After addition of the CuOx electrodes, only trace amounts of formate could be detected in the electrolyte of mature MES reactors (Figure 2c). Considering that deactivated MES effluent does evidently not affect the electrocatalytic production of formate (Figure 2c), the most likely explanation is that electrocatalytically produced formate is being consumed to acetate by the biocatalyst. Compared to co-catalytic experiments inoculated at day zero, which show a slow consumption of formate over time, mature bio-cultures consumed formate much faster, resulting in only trace amounts of formate being detected in the electrolyte (Figure 2c).

Overall, these results support co-catalytic activity between the metal- and bio-electrocatalyst, as both can be active simultaneously in the same reactor. The relationship is



syntrophic, as evident by the consumption of formate by the biocatalyst. Continuous removal of the product (i.e. formate) could improve the kinetics of CO<sub>2</sub> reduction by the metal catalyst, thus resulting in a mutualistic syntrophic relationship, as both syntrophic partners would benefit from the combination. However, this effect cannot be quantified, as the amount of formate consumed by bacteria is not known. Therefore, further distinction between mutualistic or commensalistic syntrophic relationship is not possible at this stage.

As shown in Figure 2c, up to 100 mg L<sup>-1</sup> of formate can be produced by CuOx in the presence of deactivated MES effluent, which, if fully converted, would yield 65 mg L<sup>-1</sup> of acetate (eq. VII in Figure 1). Therefore, if only syntrophic effects are considered, CuOx should have resulted in mild increase of acetate concentration by 65 mg L<sup>-1</sup>, compared to Cu-foil. Instead, acetate concentration in the presence of CuOx was much higher (900 mg L<sup>-1</sup>), compared to Cu-foil (270 mg L<sup>-1</sup>, Figure 3a). Thus, the recorded increase in acetate production observed with CuOx electrodes cannot be attributed to only syntrophic effects, but should also consider other symbiotic effects between the two catalysts, such as the increased surface roughness of CuOx for biofilm formation (Figure 4b, compared to Figure 4a), or the positive surface charge, which may improve the electronic interaction between the cathode and microorganisms for improved electron transfer.<sup>[10a]</sup> This conclusion is further substantiated by the results recorded for the two Cu-foil MES bio-reactors. As mentioned in the experimental section (see section: Testing the pure syntrophic effects of formate addition to MES), 50 mg L<sup>-1</sup> of formic acid were added at the start of the experiment in one of the duplicate Cu-foil reactors (Figure 2d), in order to simulate electrocatalytic formate production. The added substrate was depleted within the first 4 days of experiment, and did not lead to significant differences between the two duplicate reactors, either in terms of optical density during the initial stage (Figure 3c), or in terms of current evolution and acetate production for the entire duration of the experiment (Figure 2b and Figure 3a, respectively). Taken together, the improved acetate production with CuOx, and the insignificant effect of added formic acid on acetate production between the two Cu-foil reactors, indicate that symbiotic effects exist between the metal and biocatalyst, which (at least partially) explain the improved acetate production with CuOx. While the calculated acetate production during MES was higher in the presence of CuOx electrodes by approximately a 3.3-fold (Figure 3a), the calculated electron recovery to acetate was similar between reactors with CuOx and Cu-foil electrodes (Figure 3b). Increase in acetate production was therefore likely due to the 3-fold increase in current density observed with CuOx (Figure 2a), compared to Cu-foil (Figure 2b).

In addition to formate, gas products were evidently also produced with both Cu-foil and CuOx electrodes, as gas bubble formation could be observed on the surface of the electrodes. While formate, produced by the CuOx catalyst, can serve as an electron donor for MES, by comparing the amount of electron equivalents from formate production (i.e. 4.45 mmol L<sup>-1</sup> of electrons from 100 mg L<sup>-1</sup> formate) to the number of electrons incorporated into acetate by the end of the experiment (i.e.

120 mmol L<sup>-1</sup> of electrons from 900 mg L<sup>-1</sup> acetate), it is clear that formate was not the only electron donor during MES experiments reported here. Alternative sources of electrons for microbial growth and metabolism should therefore be considered, such as indirect electron transfer via H<sub>2</sub>. H<sub>2</sub> concentration was not measured during any of the experiments reported here, and therefore the exact mechanism of electron transfer to the microorganisms cannot be elucidated based on the present results. Nevertheless, consumption of formate in the presence of metabolically-active microorganisms does provide conclusive evidence of a syntrophic relationship, even though the role of hydrogen production and consumption was not investigated as part of this relationship.

### Parasitic and inhibitory effects between copper electrodes and microorganisms

Microbial activity was clearly not completely inhibited by the presence of copper electrodes in the experiments shown here, which supports that catalytic combination using these types of electrodes is possible with MES. Nevertheless, some partial inhibition or competition with biological processes may have occurred. Similarly, the growth and metabolism of microorganisms may have caused some negative symbiotic and syntrophic effects on the copper catalyst, as is discussed further in this section. While partial inhibition was not investigated, some clear differences can be observed in MES performance among the different electrodes used here, particularly with graphite felt, compared to the two copper electrodes. In the presence of graphite felt, the average concentration of acetate exceeded 2 g L<sup>-1</sup> after 29 days of inoculation, whereas the average concentration of acetate was less than 1 g L<sup>-1</sup> after 32 days in the presence of only copper electrodes (Figure 3a).

Higher acetate production with graphite felt could be due to the higher biocompatibility of this electrode material, compared to copper, in terms of biofilm attachment and toxicity. While carbonaceous materials are characterized by high biocompatibility and optimal surface properties for biofilm growth, a metallic copper surface is generally considered an antimicrobial material.<sup>[38]</sup> Thus, some inhibition of biological growth may have occurred during MES experiments with copper electrodes, particularly in the form of biofilm growing on the reduced metal electrode surface. On the contrary, during mature MES experiments, a graphite felt electrode was used for 19 days before the CuOx electrode was added in the reactor, and thereafter the graphite felt electrode remained in the reactor until the end of the experiment. Thus, a similar inhibition would not have occurred during mature MES experiments, which contained a graphite felt electrode as a more biocompatible support for biofilm attachment. Biofilm formation on the electrode during mature MES experiments was not measured with SEM. Nevertheless, similar optical density was measured in the electrolyte over time during both MES and mature MES experiments. Thus, higher acetate production during mature MES experiments was not due to higher concentration of planktonic microorganisms. It is therefore

reasonable that higher acetate production during mature MES experiments may have been due to higher biofilm formation on graphite felt electrodes.

The calculated electron recovery also differs between the two biological experiments, with an average maximum recovery of 60% in the presence of graphite, compared to an average maximum of 30% in the presence of only copper electrodes (Figure 3b). These results support that the use of copper electrodes resulted in inhibition of biological acetate production. One possible explanation for this could be the different catalytic activity between copper and graphite felt. Some reactions may be catalysed by the copper electrodes during biological experiments at  $-1.2$  V, whereas these reactions may proceed at a lower rate with a graphite electrode at  $-1.06$  V. Thus, lower acetate production during biological experiments with copper could be due to electron competition among the electrode and the microorganisms (parasitic relationship), compared to the graphite felt electrode operating at lower potential during the first 19 days of mature MES experiments.

In addition to electron competition with the copper catalyst, acetate production may have been limited during MES experiments due to other competing biological reactions. Several mechanisms employed by bacteria to minimize the toxic effects of copper have been described.<sup>[13a]</sup> These include extracellular sequestration of copper ions, metallothionein-like copper-scavenging proteins in the cytoplasm and periplasm, as well as active extrusion of copper from the cell. The total copper atom concentration was measured in the electrolyte during the first 9 days of MES experiments with CuOx and Cu-foil electrodes, and the results are shown in Figure S4 (in Supporting Information). As can be observed, for both CuOx and Cu-foil, the concentration of dissolved copper in the electrolyte at the start of the experiment was higher (i.e. up to  $550 \mu\text{g L}^{-1}$  for Cu-foil and  $400 \mu\text{g L}^{-1}$  for CuOx) compared to the expected concentration of the biological growth medium ( $7.6 \mu\text{g L}^{-1}$ ), thus indicating leaching of copper ions from the electrodes. Therefore, during MES experiments, microorganisms may have invested more energy in their defence against copper toxicity, and therefore the yield for the desired product (acetate) was low. This could have been particularly evident when copper was added at the same time as the bacteria (MES experiments). Instead, when copper is added to a pre-grown bio-culture, bacteria are likely better acclimated to reactor conditions and may therefore respond faster to the toxic effects. More bacteria are present in the mature MES reactor, compared to a reactor that was just inoculated, and therefore the toxic effect is divided and the response is amplified by the number of bacteria present. Graphite felt, still present in the reactor during experiments with mature MES cultures, may also adsorb dissolved copper ions, thus further minimizing the toxicity. Bacteria growing as biofilm on the graphite may be more protected against dissolved copper, as only the outer layer of the biofilm would experience high copper concentrations in the electrolyte, whereas diffusion limitation and active sequestration of copper in the outer layers of the biofilm would result in lower concentrations in deeper layers.

At the end of MES experiments, both Cu-foil and CuOx electrodes used here were covered with biofilm. Development of a robust electro-active biofilm on the electrode is usually one of the objectives of MES,<sup>[39]</sup> as it allows high biomass concentration and facilitates electron transfer to the microorganisms. Nevertheless, the effect of biofilm formation on the catalytic activity of the metal is unclear. Complete covering of the metal catalyst could decrease the catalytic activity of the electrode due to biofouling, as it would block the surface of the catalyst.<sup>[14]</sup> Generally, biofilm formation is considered as a negative factor for the performance of cathode electrodes, presumably by catalyst poisoning<sup>[40]</sup> and increasing the resistance of electron or mass transfer, although a previous study by Santoro and co-workers using activated carbon, iron and aminoantipyrine-based cathode electrodes has shown that biofilm coverage after 16 days did not significantly affect the cathode performance.<sup>[15]</sup> Clearly, future research on combining metal and biocatalysts should focus on the potentially negative symbiotic effect of biofilm development on the electrode, particularly for long term experiments (e.g. 32 days in this study).

#### Limitations and opportunities for catalytic cooperation between copper electrodes and MES

In this study, a pure copper electrode, thermally annealed at  $300^\circ\text{C}$  to form a CuOx layer, was used as catalyst for the production of formate from  $\text{CO}_2$ , with a maximum electron recovery of less than 1%. While gas formation was not quantified, gas bubble formation on the surface of the electrode was evident during experiments, and likely accounts for the remaining electron recovery. In order to improve the applicability of copper electrodes for co-catalytic processes, the selectivity towards the desired products should be better investigated. It has been previously shown that the electro-catalytic activity of copper electrodes can depend on the electrolyte composition, particularly the use of phosphate instead of bicarbonate-based buffer, which can drastically decrease the selectivity to formate, while increasing the selectivity to  $\text{H}_2$ .<sup>[22: 41]</sup> In an attempt to increase formate production with CuOx electrodes during MES, we have previously recommended an approach to optimize the electrolyte for formate production, by increasing bicarbonate and minimizing phosphate buffer concentration.<sup>[22]</sup> In our studies, phosphate salts in the electrolyte were used as a buffer at high concentrations ( $9 \text{ g L}^{-1}$  in total). Instead, if another buffer salt was selected, the required concentration for phosphate salts would be much lower, as is the case for other macronutrients (e.g.  $0.2 \text{ g L}^{-1}$  for  $\text{NH}_4\text{Cl}$ ). For example, a medium containing  $0.24 \text{ M}$  of  $\text{NaHCO}_3$  (i.e. within the range of concentrations typically used for metal catalysts) and only  $0.2 \text{ g L}^{-1}$  of  $\text{K}_2\text{HPO}_4$  has been previously used as electrolyte for a mixed culture of microorganisms, converting  $\text{CO}_2$  to acetate.<sup>[42]</sup> Such a bicarbonate-rich and phosphate-limited medium composition could improve the selectivity to formate during co-catalytic processes. Compared to previous studies on catalytic combination, which

use pure cultures of microorganisms to combine with metal catalysts, designing an optimal electrolyte for both catalysts may be further facilitated here, due to the adaptability of mixed cultures to a variety of ambient conditions. It has been previously shown that a mixed consortium of acetogenic microorganisms can be adapted to a bicarbonate-rich medium by sequential growth in reactors with increasing concentrations of up to  $15 \text{ g L}^{-1}$ .<sup>[43]</sup> While the acetate production rate was enhanced due to the high bicarbonate concentration, the carbon conversion efficiency exhibited the opposite effect. In addition, further increase of the concentration to  $20 \text{ g L}^{-1}$  resulted in inhibiting conditions and decreased acetate production.<sup>[43]</sup> Clearly, optimizing the electrolyte composition for a co-catalytic process requires further investigation on the effects of high bicarbonate concentration on the individual and combined catalytic reactions. Nevertheless, optimization of the electrolyte composition was not tested here, as microbial inoculum was pre-acclimated to phosphate-based medium in the parent reactors, and changes in the electrolyte composition could have resulted in unexpected changes in microbial community composition and metabolic activity.

Extensive biofilm formation on the copper electrodes observed here, contradicts previous reports with copper foam bio-cathodes with a pure culture of *Sporomusa ovata*, where only scattered and damaged cells could be observed on the electrode.<sup>[10b]</sup> However, the surprising biocompatibility of copper electrodes for biocatalysed anodic reactions has been previously shown, by comparing various metal electrodes, as well as graphite electrodes, for application in bioanodes with mixed-culture acetate-oxidizing microorganisms.<sup>[44]</sup> In fact, the authors reported higher biofilm thickness on copper ( $249 \mu\text{m}$ ) compared to graphite ( $117 \mu\text{m}$ ), which resulted in higher current generation from acetate oxidation at the two anodes. This could be due to the passivating effects of phosphate ions contained in the electrolyte solution, as well as components of the biofilm itself, which can bind metal ions and prevent toxic effects to the microorganisms.<sup>[44]</sup> For example, the release of extracellular polymeric substances (EPS) as a response to high dissolved copper concentrations has been previously shown to be employed by metal-tolerant microorganisms, during the simultaneous copper reduction and acetate production in MES experiments.<sup>[45]</sup> Interestingly, dissolved copper sequestration and EPS production were shown to be enhanced in the biofilm, compared to planktonic microorganisms.<sup>[45]</sup> Such adaptations of the microbial community to metal toxicity, particularly within the biofilm, may explain the formation of biofilm on copper electrodes observed here. More recently, the improved bioelectrocatalytic performance of anodic biofilms on copper electrodes, compared to graphite electrodes, was attributed to copper sulphides, formed due to dissolution of copper ions from the anode and sulphate reduction by microorganisms, which are incorporated as a conductive network in the biofilm, resulting in improved electrogenicity.<sup>[46]</sup> While the tolerance for mixed cultures of electro-active microorganisms to copper needs further elucidation, the findings of the present study, in agreement with the results of Schröder and co-workers,<sup>[44,46]</sup>

confirm that copper can be a suitable support material for biofilm formation during bio-electrochemical processes.

While a pure copper electrode was shown to be a suitable support for the development of cathodic biofilm, more biocompatible materials like graphite felt may improve biological growth and products selectivity. In order to employ co-catalytic processes using copper catalysts and biocatalysts, while minimizing the potentially toxic effects of copper to the biological process, copper nanoparticles could be employed, supported on more biocompatible, carbonaceous materials. Previous studies have demonstrated that copper nanoparticles supported on a carbonaceous electrode can achieve high selectivities for formate production, with reported electron recoveries of up to 80%.<sup>[47]</sup> Aside from pure copper, bimetallic catalysts or alloys of different metals could be considered, as they could increase the biocompatibility of the catalyst by decreasing the content of copper.<sup>[48]</sup> For example, a  $\text{CuSn}_3$  alloy catalyst has been recently shown to achieve 95% selectivity for formate production at high current density and low overpotential, with no evident loss of activity after 50 hours.<sup>[49]</sup> Importantly, metals such as copper and tin are much more competitive in terms of price than indium, which has been previously used for co-catalytic reactions with MES,<sup>[18-21]</sup> with an estimated price of over 20 or 8 times lower than indium, respectively.<sup>[50]</sup> Therefore, a co-catalytic process based on supported copper nanostructures or alloys of copper would be more applicable, and effectively use smaller amounts of metal catalyst, while it has the potential to increase the biocompatibility of the electrode, by using carbonaceous support materials.

As discussed in the previous section, microbial growth on copper electrodes may have resulted in decreased catalytic activity for the latter, due to blocking of the catalytic surface. Combining metal nano-catalysts on a carbonaceous support could possibly help overcome the limitation of biofilm blocking the electrode surface. Likely, microorganisms would preferentially grow on the more biocompatible parts of the electrode, thus prevent covering of the catalytically-active surface (i.e. metals). For example, Tian and co-workers report that  $\text{H}_2$  catalytic activity was retained after 14 days of MES experiments, despite biofilm formation on the carbonaceous electrodes with supported molybdenum carbide nanostructures after 30 days of MES operation.<sup>[11]</sup> This could be due to microbial growth on the carbon support, instead of the catalytic nanostructures, which would prevent biofouling of the catalytically active sites, and thus retaining catalytic activity for  $\text{H}_2$  evolution. However, as both the catalyst dispersion and biofilm formation appear to be rather heterogeneous on the carbon support, based on the SEM images provided, the location of the biofilm in relation to the catalyst cannot be further elucidated. Therefore, more research would be required to reveal the optimal architecture of a biocompatible and catalytically-active metal electrodes to combine with MES.

## Conclusion

We have shown that metabolic cooperation is possible between a copper electrocatalyst and a mixed culture of naturally occurring MES biocatalysts, including formate as metabolic intermediate. Both catalysts appear active upon combination in one reactor. Syntrophic effects between the two catalysts were evident, as formate was produced by CuOx and depleted in the presence of microorganisms, whereas depletion did not occur in the absence of microorganisms. In addition to syntrophic (i.e. metabolic), other symbiotic effects were also observed upon combining the two catalysts. Specifically, compared to an unmodified copper foil electrode, CuOx electrodes resulted in a 3-fold increase in current density during MES experiments, accompanied by an equivalent increase in acetate production, as a result of symbiotic effects between the two catalysts. In spite its antimicrobial role, copper allowed the formation of biofilm on the surface of the electrode.

The effect of biofilm coverage on the catalytic activity of copper was not investigated (i.e. blocking of active sites on the electrode or electron competition). Nevertheless, it was indicated that the presence of microorganisms in the electrolyte does not affect the long-term catalytic activity of copper for CO<sub>2</sub> reduction to formate. Overall, this study shows that there is potential for combining copper and biocatalyst in one reactor.

Considering this unprecedented biocompatibility of a pure copper electrode as an MES bio-cathode electrode, some strategies are discussed to further improve the performance of co-catalytic concepts based on copper catalysts, including the optimization of the electrode structure and electrolyte composition.

## Experimental Section

### Electrode preparation

Copper foil (Cu-foil), titanium and platinum wires were purchased from Salomon's Metalen B.V., the Netherlands. Copper foil was cut in square pieces (2×2×0.01 cm), and each was connected to a titanium wire current collector (Ø=0.8 mm), by applying mechanical pressure to clamp the wire to the foil. The thus prepared electrodes (i.e. Cu-foil connected to Ti wire) were pre-treated by sonication in acetone (99.8%) for 30 minutes, followed by sonication in iso-propanol (99.95%) and finally in demi water, each for 30 minutes, to remove organic contaminants from the surface. Electrodes were rinsed with demi water between sonication in different solvents. Hereafter the electrodes were electropolished in concentrated phosphoric acid (85%) at a current of +2.08 A for one minute, where copper foil was used as the counter electrode. Finally, the electrodes were rinsed with milli-Q water and dried under dry N<sub>2</sub> flow at 25 °C. Electropolished Cu-foil electrodes were annealed in a muffle static air oven (Nabertherm P 330) at 300 °C for 12 hours, to develop a surface copper oxide layer, as has been previously described.<sup>[51]</sup> These copper oxide (CuOx) electrodes were manufactured in at least quadruplicates.

For some experiments, graphite felt (4mm thick, CTG Carbon GmbH, Germany) was used as a cathode electrode. Prior to electrode manufacture, graphite felt was treated overnight in 33% nitric acid at 25 °C, in order to increase the hydrophilicity of the

material, and thereafter washed with demi water, until the effluent pH was neutral. Electrodes were prepared using a dry piece of graphite felt (3×4×0.4 cm), by passing a titanium wire current collector through the felt. For all the cathode electrodes, the projected surface area was calculated based on dimensions. The calculated surface area was 8 cm<sup>2</sup> for both Cu-foil and CuOx electrodes (i.e. 2 sides of 4 cm<sup>2</sup> each). For graphite felt, a three-dimensional electrode, the projected surface area is typically calculated based on one side,<sup>[52]</sup> thus corresponding to 12 cm<sup>2</sup>. The formulas used for calculations are shown in Supporting Information (formula I and II, section S5).

For electrochemical experiments, anode (counter) electrodes were prepared by wrapping 7 cm of platinum wire (99.95% and Ø=0.3 mm) on the edge of a piece of titanium wire current collector. The reference electrode used for all electrochemical tests was Ag/AgCl (3 M KCl), and all potentials in this paper are reported against that electrode. An IVIUM n-stat potentiostat (IVIUM technologies B.V., the Netherlands) was used for all electrochemical techniques.

### (Bio)electrochemical experiments

In order to determine the symbiotic or syntrophic effects between copper electrodes and microorganisms, several chronoamperometry experiments were performed, as described in Table 2.

Chronoamperometry was performed in a 3-electrode, 2-compartment electrochemical H-type reactor, with a Nafion cation-exchange membrane (projected surface area 11.3 cm<sup>2</sup>) separating the anode and cathode compartments, with a total volume of 310 ml each. An image of the reactor is shown in Figure S6 (in Supporting Information). All chronoamperometry experiments were performed at a cathode potential of -1.2 V, unless otherwise indicated. The anolyte (250 ml) was phosphate buffer, and the catholyte (220 ml) was autoclaved biological growth medium. The electrolyte composition is shown in Table 3. All electrochemical tests were performed at 25 °C. The catholyte was continuously flushed with pure CO<sub>2</sub> gas (50 mlmin<sup>-1</sup>) during electrochemical experiments, maintaining a catholyte pH of 6.6–6.7 throughout the experiment, unless otherwise indicated. The catholyte sampling frequency was varied among experiments (1–4 days). Excess gas was vented to the air via a water lock. Gas products were therefore not analysed.

**Table 2.** Description of electrochemical experiments. Abbreviations: CuOx (copper oxide), Cu-foil (electropolished copper foil). Unless otherwise indicated, both biocatalysts and electrocatalysts are added in the reactor at the start of the experiment, before applying cathode potential. All experiments were performed in duplicate (2x), but some results were excluded due to biological contamination in the reactor (1x\*). Formic acid was added in the catholyte of one MES Cu-foil reactor, but not the other, and therefore these reactors are not exact duplicates (2x\*\*).

Code name	Electrocatalyst [& replicates]	Biocatalyst	Duration
CES	CuOx (1x*) Cu-foil (2x)	No	21 days 10 days
MES	CuOx (2x) Cu-foil (2x**)	Yes	32 days
deactivated MES	CuOx (1x*) Cu-foil (1x*)	Yes, deactivated	21 days
mature MES	Graphite felt (29 days) & CuOx (added on day 19) (2x)	Yes	29 days



**Table 3.** Composition of electrolytes.

Component	Growth medium	Phosphate buffer
Na <sub>2</sub> HPO <sub>4</sub>	6 g L <sup>-1</sup>	6 g L <sup>-1</sup>
KH <sub>2</sub> PO <sub>4</sub>	3 g L <sup>-1</sup>	3 g L <sup>-1</sup>
NH <sub>4</sub> Cl	0.2 g L <sup>-1</sup>	–
MgCl <sub>2</sub> ·6H <sub>2</sub> O	0.04 g L <sup>-1</sup>	–
CaCl <sub>2</sub>	0.015 g L <sup>-1</sup>	–
FeCl <sub>3</sub> ·6H <sub>2</sub> O	1.5 mg L <sup>-1</sup>	–
H <sub>3</sub> BO <sub>3</sub>	0.15 mg L <sup>-1</sup>	–
CuSO <sub>4</sub> ·5H <sub>2</sub> O	0.03 mg L <sup>-1</sup>	–
KI	0.18 mg L <sup>-1</sup>	–
MnCl <sub>2</sub> ·4H <sub>2</sub> O	0.12 mg L <sup>-1</sup>	–
Na <sub>2</sub> MoO <sub>4</sub> ·2H <sub>2</sub> O	0.06 mg L <sup>-1</sup>	–
ZnSO <sub>4</sub> ·7H <sub>2</sub> O	0.12 mg L <sup>-1</sup>	–
CoCl <sub>2</sub> ·6H <sub>2</sub> O	0.15 mg L <sup>-1</sup>	–
NiCl <sub>2</sub> ·6H <sub>2</sub> O	0.023 mg L <sup>-1</sup>	–
ethylenediaminetetraacetic acid (EDTA)	10 mg L <sup>-1</sup>	–

### Selecting an appropriate duration for electrochemical experiments

Electrochemical experiments with metal catalysts are typically short (i.e. minutes to hours, as reported for example by Jermann and Augustynski<sup>[53]</sup> or Li and Kanan<sup>[51]</sup>), whereas MES experiments are commonly performed for longer time (i.e. days to months, as reported for example by Nie and co-workers<sup>[12]</sup> or Jourdin and co-workers<sup>[54]</sup>). To understand the dynamics of formate production and consumption over time, at a time-scale relevant for MES, all electrochemical experiments were performed for multiple days. During MES experiments with CuOx, the electrocatalytically-produced formate was depleted after 21 days. Therefore, abiotic experiments were performed for 21 days, in order to investigate if a similar depletion of formate would take place in the absence of microorganisms. Instead, biological experiments were carried out for longer time periods (i.e. 32 days), in order to illustrate the effects of different electrodes on mature MES communities. No formate production was detected during CES experiments with Cu-foil electrodes, therefore these reactors were not operated for 21 days, but were discontinued on day 10, as is shown in Table 2.

### Source of microorganisms

Two MES reactors with mixed communities of microorganisms had been operated for three years at a cathode potential of  $-1.06$  V, with graphite felt cathodes, under the same conditions as described above (see section: (Bio)electrochemical experiments; data not shown). Inoculum for these reactors was obtained from a previously-described bio-reactor.<sup>[55]</sup> These “parent” reactors were used as source of microorganisms for all biological experiments reported in this paper.

At the start of every biological experiment, reactors were inoculated with microorganisms from the parent MES reactors. Inoculum was prepared from a liquid sample, twice centrifugated at 6000 rpm for 10 min and re-suspended in fresh biological growth medium.

### Deactivation of microorganisms for abiotic experiments (Deactivated MES tests)

Some electrochemical experiments were performed with deactivated microorganisms in the electrolyte. Metabolic deactivation was achieved by heating the effluent of parent reactors at 60 °C for 30 min.<sup>[56]</sup> Deactivated biological effluent was allowed to cool

down, and then used directly as medium for abiotic chronoamperometry experiments (as described above, see section: (Bio) electrochemical experiments). This experiment allowed to study the pure symbiotic effects of microorganisms on the metal catalyst (e.g. blocking/poisoning of catalyst surface), without underestimating formate production, as a result of active microbial metabolism (i.e. formate consumption by microorganisms).

### Testing the effect of copper electrodes on mature MES communities (Mature MES tests)

Batch production processes based on microbial growth are typically characterized by different phases, including a lag phase at the start, followed by acclimation and exponential growth, and concluding with a static and death phase.<sup>[57]</sup> To better understand the symbiotic and syntrophic effects of copper at different stages of microbial growth, two MES reactors were used to test the co-catalytic activity of CuOx and a mature MES community. Reactors were inoculated and operated with graphite felt cathodes at  $-1.06$  V, as previously described for parent reactors (see section: Source of microorganisms). 18 days after inoculation and after acetate production had started, CuOx electrodes were added in these MES reactors, and thereafter the potentiostat was restarted, controlling the CuOx electrodes at  $-1.2$  V. The graphite felt electrodes were disconnected from the potentiostat but remained in the reactors, so as not to remove the microorganisms grown as biofilm on the electrodes during the first 18 days.

### Testing the pure syntrophic effects of formate addition to MES (MES tests with Cu-foil)

To study the pure syntrophic effects of formate production on microorganisms, formic acid (50 mg L<sup>-1</sup>) was added at the start of the experiment in the electrolyte of one of the two MES reactors with Cu-foil. Adding formic acid was intended to simulate the production of formate with CuOx in this Cu-foil reactor. By comparing the reactor containing formic acid to the reactor that did not, while all other parameters between the two reactors remained the same (e.g. electrode type, current density), the syntrophic effects of (simulated) formate production on MES could be revealed. Formic acid was used (instead of formate salts) to keep the composition of the electrolyte the same between the two reactors.

Due to the buffering capacity of the electrolyte, formic acid addition did not cause deviation in terms of pH among the two Cu-foil reactors ( $6.79 \pm 0.021$  for Cu-foil and  $6.84 \pm 0.021$  for CuOx reactors after 24 hours). Moreover, formic acid addition did not cause deviation between the two Cu-foil reactors in terms of current and optical density, as is shown in Supporting Information (Figure S7). The added formic acid was depleted by day 4, likely due to evaporation, oxidation at the anode, and/or biological consumption. Therefore, the reactors were treated as duplicates from day 7 onwards, and average values are reported in the rest of this manuscript.

### Analytical techniques and calculations

Surface characterization of the copper oxide catalyst was performed using Scanning electron microscopy (SEM, FEI Magellan 400 FESEM) with energy dispersive X-ray spectroscopy (EDS, Oxford Instruments) equipped with an Everhart-Thornley Detector, at 2.00 kV voltage and 13 pA current, before and after electrochemical tests, as well as on biofilm-covered electrodes, at the end of the experiments.

In order to perform SEM-EDX on biofilm-covered electrodes, fixation of biological structures was performed with glutaraldehyde. Electrodes were removed from the biological reactors at the end of the experiment, and were stored in 2.5% glutaraldehyde solution in growth medium. Biofilm-covered electrodes were treated in ethanol solutions with incrementally increasing concentration (from 10% to 100%) to remove water, and thereafter dried using Critical Point Drying. To allow visualization of the biofilm with SEM, samples were coated with 12 nm Tungsten before analysis.

Gas chromatography (Agilent technologies) using flame ionization detection (GC-FID) was used to analyse liquid products from chronoamperometry experiments in catholyte samples (C2-C8 volatile fatty acids and medium-chain fatty acids, C1-C6 alcohols), as previously described.<sup>[8]</sup> The concentration of formate was measured with high performance liquid chromatography (HPLC), with refractive index (RI) and UV detection (column specification: Aminex HPX-87H, 300×7.8 mm, BioRad 1225-0140). Inductively coupled plasma optical emission spectroscopy (ICP-OES) was used to quantify the amount of copper ions that leached from the cathode over time during electrochemical experiments.

Optical density (Abs) was measured in catholyte samples at 660 nm to monitor the growth of planktonic microorganisms in biological reactors (HACH LANGE DR3900 spectrophotometer). Dissolved ammonium concentration was measured over time in the catholyte to estimate nutrient consumption by both planktonic and biofilm-forming microorganisms in MES reactors (HACH LANGE DR3900 spectrophotometer, HACH LCK 304 Ammonium cuvette test). At the end of MES experiments, the microbial community composition of one replicate reactor with CuOx electrode was analysed. The methodology and results are shown in Supporting Information (Figure S8).

The current densities (in mAcm<sup>-2</sup>) reported throughout this manuscript were calculated based on the defined projected electrode surface area (8 cm<sup>2</sup> for Cu-foil and 12 cm<sup>2</sup> for graphite felt), as shown in Supporting Information (formula III, section S5).

For electrochemical experiments, electron recovery (%) was calculated between consecutive sampling points, and the corresponding calculations are shown in Supporting Information (formula IV, section S5). Changes in volume and dilution due to refreshing of the reaction medium were corrected for, when calculating the electron recoveries (formula V, section S5 in Supporting Information).

## Acknowledgements

We gratefully acknowledge the Wageningen Institute for Environment and Climate Research (WIMEK), the Graduate School of Food Technology, Agrobiotechnology, Nutrition and Health Sciences (VLAG) of Wageningen University, as well as TKI Watertechnologie, Magneto special anodes B.V. and W&F Magneto B.V. for funding this work.

## Conflict of Interest

The authors declare no conflict of interest.

**Keywords:** biocatalysis · carbon dioxide fixation · electrocatalysis · metabolic intermediates · microbial electrosynthesis

- [1] C. Hepburn, E. Adlen, J. Beddington, E. A. Carter, S. Fuss, N. Mac Dowell, J. C. Minx, P. Smith, C. K. Williams, *Nature*. **2019**, *575*, 87–97.
- [2] E. Alper, O. Yuksel Orhan, *Petroleum*. **2017**, *3*, 109–126.
- [3] R. L. House, N. Y. M. Iha, R. L. Coppo, L. Alibabaei, B. D. Sherman, P. Kang, M. K. Brennaman, P. G. Hoertz, T. J. Meyer, *J. Photochem. Photobiol. C* **2015**, *25*, 32–45.
- [4] L. Jourdin, J. Sousa, N. van Stralen, D. P. B. T. B. Strik, *Appl. Energy*. **2020**, *279*, 115775.
- [5] K. Rabaey, R. A. Rozendal, *Nat. Publ. Gr.* **2010**, *8*, 706–716.
- [6] S. W. Ragsdale, E. Pierce, *Biochim. Biophys. Acta Proteins Proteomics* **2008**, *1784*, 1873–1898.
- [7] a) D. R. Lovley, K. P. Nevin, *Curr. Opin. Biotechnol.* **2013**, *24*, 385–390; b) P.-L. Tremblay, T. Zhang, *Front. Microbiol.* **2015**, *6*, 201.
- [8] L. Jourdin, S. M. T. Raes, C. J. N. Buisman, D. P. B. T. B. Strik, *Front. Energy Res.* **2018**, *6*, 7.
- [9] V. Balan, *ISRN Biotechnol.* **2014**, *2014*, 1–31.
- [10] a) T. Zhang, H. Nie, T. S. Bain, H. Lu, M. Cui, O. L. Snoeyenbos-West, A. E. Franks, K. P. Nevin, T. P. Russell, D. R. Lovley, *Energy Environ. Sci.* **2013**, *6*, 217–224; b) N. Aryal, L. Wan, M. H. Overgaard, A. C. Stoot, Y. Chen, P.-L. Tremblay, T. Zhang, *Bioelectrochemistry*. **2019**, *128*, 83–93; c) F. Kracke, A. B. Wong, K. Maegaard, J. S. Deutzmann, M. A. Hubert, C. Hahn, T. F. Jaramillo, A. M. Spormann, *Commun. Chem.* **2019**, *2*, 45.
- [11] S. Tian, H. Wang, Z. Dong, Y. Yang, H. Yuan, Q. Huang, T. Song, J. Xie, *Biotechnol. Biofuels*. **2019**, *12*, 71.
- [12] H. Nie, T. Zhang, M. Cui, H. Lu, D. R. Lovley, T. P. Russell, *Phys. Chem. Chem. Phys.* **2013**, *15*, 14290–14294.
- [13] a) G. Grass, C. Rensing, M. Solioz, *Appl. Environ. Microbiol.* **2011**, *77*, 1541–1547; b) C. E. Santo, E. W. Lam, C. G. Elowsky, D. Quaranta, D. W. Domaille, C. J. Chang, G. Grass, *Appl. Environ. Microbiol.* **2011**, *77*, 794–802; c) S. Prabhu, E. K. Poulouse, *Int. Nano Lett.* **2012**, *2*, 32; d) S. L. Warnes, V. Caves, C. W. Keevil, *Environ. Microbiol.* **2012**, *14*, 1730–1743.
- [14] G. Mohanakrishna, S. Kalathil, D. Pant, *Microbial Fuel Cell* (Eds.: D. Das), Springer International Publishing, Cham, **2018**, pp. 209–227.
- [15] C. Santoro, A. Serov, C. W. N. Villarrubia, S. Stariha, S. Babanova, K. Artyushkova, A. J. Schuler, P. Atanassov, *Sci. Rep.* **2015**, *5*, 16596.
- [16] L. Jourdin, Y. Lu, V. Flexer, J. Keller, S. Freguia, *ChemElectroChem*. **2016**, *3*, 581–591.
- [17] O. Yishai, S. N. Lindner, J. Gonzalez de la Cruz, H. Tenenboim, A. Bar-Even, *Curr. Opin. Chem. Biol.* **2016**, *35*, 1–9.
- [18] H. Li, P. H. Opgenorth, D. G. Wernick, S. Rogers, T.-Y. Wu, W. Higashide, P. Malati, Y.-X. Huo, K. M. Cho, J. C. Liao, *Science* **2012**, *335*, 1596–1596.
- [19] Y. Tashiro, S. Hirano, M. M. Matson, S. Atsumi, A. Kondo, *Metab. Eng.* **2018**, *47*, 211–218.
- [20] R. Hegner, K. Neubert, C. Kroner, D. Holtmann, F. Harnisch, *ChemSusChem*. **2020**, *13*, 5295–5300.
- [21] I. S. Al Rowaihi, A. Paillier, S. Rasul, R. Karan, S. W. Grötzinger, K. Takanabe, J. Eppinger, *PLoS One*. **2018**, *13*, e0196079.
- [22] K.-R. Chatzipanagiotou, L. Jourdin, C. J. N. Buisman, D. P. B. T. B. Strik, J. H. Bitter, *ChemCatChem*. **2020**, *12*, 3900–3912.
- [23] X. Zhang, S. Guo, K. A. Gandionco, A. M. Bond, J. Zhang, *Mater. Today* **2020**, *7*, 100074.
- [24] a) M. Sarioglu, S. Akkoyun, T. Bisgin, *Desalin. Water Treat.* **2010**, *23*, 55–60; b) V. Ochoa-Herrera, G. León, Q. Banihani, J. A. Field, R. Sierra-Alvarez, *Sci. Total Environ.* **2011**, *412–413*, 380–385; c) A. Ogawa, H. Kanematsu, K. Sano, Y. Sakai, K. Ishida, I. Beech, O. Suzuki, T. Tanaka, *Materials (Basel)*. **2016**, *9*, 632.
- [25] T. E. Norgate, S. Jahanshahi, W. J. Rankin, *J. Cleaner Prod.* **2007**, *15*, 838–848.
- [26] W. Yang, B. Vogler, Y. Lei, T. Wu, *Environ. Sci.: Water Res. Technol.* **2017**, *3*, 1143–1151.
- [27] M. Gattrell, N. Gupta, A. Co, *J. Electroanal. Chem.* **2006**, *594*, 1–19.
- [28] K. D. de Leeuw, S. M. de Smit, S. van Oossanen, M. J. Moerland, C. J. N. Buisman, D. P. B. T. B. Strik, *ACS Sustainable Chem. Eng.* **2020**, *8*, 8184–8194.
- [29] S. M. T. Raes, L. Jourdin, C. J. N. Buisman, D. P. B. T. B. Strik, *ChemistrySelect*. **2020**, *5*, 9127–9133.
- [30] M. Roghair, T. Hoogstad, D. P. B. T. B. Strik, C. M. Plugge, P. H. A. Timmers, R. A. Weusthuis, M. E. Bruins, C. J. N. Buisman, *Environ. Sci. Technol.* **2018**, *52*, 1496–1505.

- [31] a) F. Chang, S. Lo, C. Ko, *Sep. Purif. Technol.* **2007**, *53*, 49–56; b) C. Cocchiara, S. Dorneanu, R. Inguanta, C. Sunseri, P. Ilea, *J. Cleaner Prod.* **2019**, *230*, 170–179; c) K. Liu, J. Yang, H. Hou, S. Liang, Y. Chen, J. Wang, B. Liu, K. Xiao, J. Hu, H. Deng, *Environ. Sci. Technol.* **2019**, *53*, 2748–2757.
- [32] G. Castro-León, E. Baquero-Quinteros, B. G. Loor, J. Alvear, D. E. Montesdeoca Espín, A. De La Rosa, C. Montero-Calderón, *Sustainability* **2020**, *12*, 9849.
- [33] D. Kubička, J. Horáček, *Appl. Catal. A* **2011**, *394*, 9–17.
- [34] M. I. Alam, S. Gupta, E. Ahmad, M. A. Haider in *Sustainable Catalytic Processes* (Eds.: B. Saha, M. Fan, J. Wang), Elsevier, Amsterdam **2015**, pp. 157–177.
- [35] M. Besson, P. Gallezot, *Catal. Today* **2003**, *81*, 547–559.
- [36] a) N. C. Marziano, L. Ronchin, C. Tortato, A. Vavasori, M. Bortoluzzi, *J. Mol. Catal. A* **2008**, *290*, 79–87; b) Y. Huang, Y. Deng, A. D. Handoko, G. K. L. Goh, B. S. Yeo, *ChemSusChem* **2018**, *11*, 320–326; c) K. R. Phillips, Y. Katayama, J. Hwang, Y. Shao-Horn, *J. Phys. Chem. Lett.* **2018**, *9*, 4407–4412; d) Y. Deng, Y. Huang, D. Ren, A. D. Handoko, Z. W. Seh, P. Hirsunsi, B. S. Yeo, *ACS Appl. Mater. Interfaces* **2018**, *10*, 28572–28581.
- [37] J. S. Deutzmann, M. Sahin, A. M. Spormann, *mBio* **2015**, *6*, e00496-15.
- [38] M. Vincent, R. E. Duval, P. Hartemann, M. Engels-Deutsch, *J. Appl. Microbiol.* **2018**, *124*, 1032–1046.
- [39] F. Ameen, W. A. Alshehri, S. Al Nadhari, *ACS Sustainable Chem. Eng.* **2020**, *8*, 311–318.
- [40] E. Martin, B. Tartakovsky, O. Savadogo, *Electrochim. Acta* **2011**, *58*, 58–66.
- [41] D. Ren, Y. Deng, A. D. Handoko, C. S. Chen, S. Malkhandi, B. S. Yeo, *ACS Catal.* **2015**, *5*, 2814–2821.
- [42] S. A. Patil, J. B. A. Arends, I. Vanwonterghem, J. van Meerbergen, K. Guo, G. W. Tyson, K. Rabaey, *Environ. Sci. Technol.* **2015**, *49*, 8833–8843.
- [43] G. Mohanakrishna, I. M. Abu Reesh, K. Vanbroekhoven, D. Pant, *Sci. Total Environ.* **2020**, *715*, 137003.
- [44] A. Baudler, I. Schmidt, M. Langner, A. Greiner, U. Schröder, *Energy Environ. Sci.* **2015**, *8*, 2048–2055.
- [45] a) Y. Qian, L. Huang, P. Zhou, F. Tian, G. Li Puma, *Sci. Total Environ.* **2019**, *666*, 114–125; b) J. Hou, L. Huang, P. Zhou, Y. Qian, N. Li, *Chemosphere* **2020**, *243*, 125317.
- [46] L. Beuth, C. P. Pfeiffer, U. Schröder, *Energy Environ. Sci.* **2020**, *13*, 3102–3109.
- [47] a) J. Qiao, M. Fan, Y. Fu, Z. Bai, C. Ma, Y. Liu, X.-D. Zhou, *Electrochim. Acta* **2015**, *153*, 559–565; b) X. Zhu, K. Gupta, M. Bersani, J. A. Darr, P. R. Shearing, D. J. L. Brett, *Electrochim. Acta* **2018**, *283*, 1037–1044; c) X. Zhang, Y. Zhang, F. Li, C. D. Easton, A. M. Bond, J. Zhang, *Nano Res.* **2018**, *11*, 3678–3690; d) T. Shinagawa, G. O. Larrazábal, A. J. Martín, F. Krumeich, J. Pérez-Ramírez, *ACS Catal.* **2018**, *8*, 837–844; e) R. García-Muelas, F. Dattila, T. Shinagawa, A. J. Martín, J. Pérez-Ramírez, N. López, *J. Phys. Chem. Lett.* **2018**, *9*, 7153–7159; f) U. Legrand, R. Boudreault, J. L. Meunier, *Electrochim. Acta* **2019**, *318*, 142–150.
- [48] L. Zhu, J. Elguindi, C. Rensing, S. Ravishankar, *Food Microbiol.* **2012**, *30*, 303–310.
- [49] X. Zheng, Y. Ji, J. Tang, J. Wang, B. Liu, H. Steinrück, K. Lim, Y. Li, M. F. Toney, K. Chan, Y. Cui, *Nat. Catal.* **2019**, *2*, 55–61.
- [50] <https://www-statista-com.ezproxy.library.wur.nl>, accessed on 12 April 2021.
- [51] C. W. Li, M. W. Kanan, *J. Am. Chem. Soc.* **2012**, *134*, 7231–7234.
- [52] M. Sharma, S. Bajracharya, S. Gildemyn, S. A. Patil, Y. Alvarez-Gallego, D. Pant, K. Rabaey, X. Dominguez-Benetton, *Electrochim. Acta* **2014**, *140*, 191–208.
- [53] B. Jermann, J. Augustynski, *Electrochim. Acta* **1994**, *39*, 1891–1896.
- [54] L. Jourdin, S. Freguia, B. C. Donose, J. Chen, G. G. Wallace, J. Keller, V. Flexer, *J. Mater. Chem. A* **2014**, *2*, 13093–13102.
- [55] L. Jourdin, T. Grieger, J. Monetti, V. Flexer, S. Freguia, Y. Lu, J. Chen, M. Romano, G. G. Wallace, J. Keller, *Environ. Sci. Technol.* **2015**, *49*, 13566–13574.
- [56] S. Xu, H. Liu, Y. Fan, R. Schaller, J. Jiao, F. Chaplen, *Appl. Microbiol. Biotechnol.* **2012**, *93*, 871–880.
- [57] R. E. Buchanan, *J. Infect. Dis.* **1918**, *23*, 109–125.

---

Manuscript received: March 7, 2021  
Revised manuscript received: April 26, 2021  
Accepted manuscript online: April 29, 2021